2009 American Control Conference
Hyatt Regency Riverfront, St. Louis, MO, USA
June 10-12, 2009

Source Seeking for a Joukowski Foil Model of Fish Locomotion

Jennie Cochran, Scott D. Kelly, Hailong Xiong, and Miroslav Krstic

Abstract— **We continue with the study of fish-like underwater source seeking initiated in a companion paper where we considered a three-rigid-link fish model. In this paper we consider a more realistic fish model based on a Joukowski airfoil which has only one degree of freedom in its movement, and thus relies on vortex shedding to move through a perfect fluid. Both the propulsion problem and the source seeking problem are solved by employing the same sinusoidal perturbation input—the flapping of the fish's tail. The fish converges to the signal source despite being unaware of it's position, the source's position, and the spatial distribution of the source.**

I. Introduction

This paper addresses GPS-denied source seeking problems for underwater vehicles which, in order to move forward, employ periodic shape deformations similar to fish movement. The motivation for this work comes from our previous work on source seeking for the nonholonomic unicycle with constant forward velocity [3], [4]. In that work we use the extremum seeking method to design a control law which drives the vehicle to the vicinity of a source.

In a companion paper [2] we address the source seeking problem for a three-link model of fish in perfect fluid. This is a nonlinear model with only four states but with an extremely complex right hand side and with an output map which is infinite dimensional (the 'fluid field'). The model has two inputs, at each of the two joints of the three-link structure. The extremum seeking guides the three-link fish to the unknown location of the measured signal.

In this paper we consider a more complex and more realistic fish model developed in [22] (and studied in [11]), employing a Joukowski airfoil representation, which has only one degree of freedom in its movement and relies on vortex shedding to move through a perfect fluid and to achieve steering. We study how to use a combination of two basic "gaits," the periodic shape deformations that produce forward and turning motions, to enable, with the help of feedback, the fish to move towards the signal source.

Much work has been done in the area of modelling fish movement - both for the understanding of fluid dynamics and for the purpose of building more efficient vehicles that operate underwater. The studies presented in [6], [9], [20], [1], [10], [18], [21] have all examined locomotion by swimming and the role of vortices. References [7], [22], [11], [5] have taken the lessons learned from this previous work and extended it to the development of computational fish models in fluid systems. The model developed in [22], [11] spans the gap between studies which look at deformable bodies moving through a fluid without the use of vortex shedding and studies examining systems with rigid bodies and vortices. Many research groups, including [19], [12], [11], [14], [8], have developed underwater vehicles modelled after biological entities which use sinusoid-dominated movements to propel the vehicle forward. In related work, [16] and references therein have studied stabilization of vortex shedding—an area with useful ideas for vehicle control.

A common theme in fish locomotion is the periodic movement of the body. This brings the extremum seeking method to mind as it employs periodic inputs to probe a signal field and achieve real-time non-model based optimization. We combine the natural gait of the fish model with the extremum seeking. By marrying the requirements of *propulsion* and *optimization*, we solve the source seeking problem in an extremely simple, biologically plausible manner.

We start in Section II with a recap of equations of motion in a perfect fluid, followed, in Section III-A, by a presentation of an ODE model of Joukowski foil motion in a field of point vortices. In Section III-B we review the basic Joukowski fish gaits and in Sections III-C and III-C introduce and test our source seeking and path following designs.

II. Equations of Motion in a Perfect Fluid

The fluid is considered to be inviscid (no viscosity) and incompressible. The fluid particles may slip along the boundaries of the solid but cavities are not allowed to form in the fluid nor at the interface. The fluid is assumed to be at rest at infinity. In [22], vorticity is shed from the trailing edge of the airfoil in the form of point vortices. Away from the shed point vortices, the fluid is assumed to remain irrotational at all time. In this case, the configuration space of the body-fluid system can be identified with that of the submerged body and the position of the shed point vortices.

The fluid velocity field $\mathbf{u}$, in the fluid domain excluding the body and point vortices when accounted for, can be expressed in term of a potential function ϕ as $\mathbf{u} = \nabla\phi$. Incompressibility implies that $\nabla^2\phi = 0$. The boundary conditions result from the two assumptions that the fluid is at rest at infinity and that fluid particles may slip along the body surface, and are expressed as $\nabla\mathbf{u}|_\infty = 0$ and $\mathbf{u}\cdot\mathbf{n} = \dot{\mathcal{B}}|_{\mathcal{S}}\cdot\mathbf{n}$, where $\mathcal{B}$ is the fish body and $\mathcal{S}$ is the surface of the body (touching the fluid). In the Joukowski airfoil model [22], [11], ϕ is a function of the configuration and velocity of the body as well as the position of the shed point vortices and is obtained in closed form using tools from complex analysis.

J. Cochran and M. Krstic are with the Department of Mechanical and Aerospace Engineering, University of California, San Diego, La Jolla, CA 92093, jcochran@ucsd.edu

S. D. Kelly is with the faculty of Mechanical Engineering and Engineering Science, University of North Carolina at Charlotte, 9201 University City Blvd, Charlotte, NC 28223

H. Xiong is with the Department of Mechanical and Industrial Engineering, University of Illinois at Urbana-Champaign, Urbana, IL 61801

This work was supported by an NDSE Graduate fellowship and NSF.

The kinetic energy of the fluid, T_f, is defined as $T_f = \frac{1}{2}\int_{\mathcal{D}} \mathbf{u}^2 dv$, where $\mathcal{D}$ is the fluid domain (excluding singularities present in the form of point vortices) and dv is the standard volume element. Using Green's theorem, T_f is rewritten as $T_f = -\frac{1}{2}\int_{\partial S} \phi \nabla\phi \cdot \mathbf{n} ds$, where ∂S is the surface of the fish body and $\mathbf{n}$ is the unit normal into the fluid. The xpression for T_f is given in Section III.

The equations governing the net locomotion of the fish can be viewed as variations of Kirchhoff's equations for the motion of a rigid body in an ideal fluid (see [13])

$$\frac{d\mathbf{L}}{dt} + \Omega \mathbf{k} \times \mathbf{L} = 0 \quad (1)$$

$$\frac{dA}{dt} + \mathbf{k} \cdot ([U\ V]^T \times \mathbf{L}) = 0 \quad (2)$$

where $\mathbf{L}$ and A are the linear and angular momenta of the body-fluid system and U, V, and Ω are the translational and rotational velocities associated with a net locomotion of the body. The variables $\mathbf{L}$, A, U, V, Ω are expressed in a body frame moving with the fish. The linear and angular momenta $\mathbf{L}$ and A are obtained by differentiating the kinetic energy $\mathbf{L} = \begin{bmatrix} \frac{\partial T}{\partial U} & \frac{\partial T}{\partial V} \end{bmatrix}^T, A = \frac{\partial T}{\partial \Omega}$. The theme of the derivations is conservation of momentum and starting the system from rest, which implies $\mathbf{L} = 0$ and $A = 0$ for all time. This allows one to solve for U, V, and Ω at each time step and then integrate to derive the locomotion of the fish.

III. Locomotion and Source Seeking for a Joukowski Foil Fish

We now move to the discussion of locomotion for a deformable Joukowski foil. [22], [11] have used the Joukowski transformation, a class of conformal maps, to study a fish modelled as an airfoil. The transformation

$$z = F(\zeta) = \zeta + \zeta_c + \frac{\alpha}{\zeta + \zeta_c} \quad (3)$$

allows the parameterization of a circle $\zeta = r_c e^{i\theta}$ in the ζ-plane to describe an airfoil in the $z = x + iy$ plane. The parameters $\zeta_c = \zeta_x + i\zeta_y \in \mathbb{C}$ and $\alpha \in \mathbb{R}$ determine the foil shape. Varying the imaginary part $\Im\{\zeta_c\} = \zeta_y$ while enforcing the constraint $r_c = |\zeta_c - \alpha|$ with r_c constant, as is done in [22], [11] and this paper, causes the camber of the foil to vary as well. This variation allows for one degree of freedom, which, by itself, will not allow the fish to make forward progress in a potential flow. To counter this, [22], [11] add discrete point vortices to the system, modelled after vortex shedding by actual fish. (The potential function in this case encompasses the domain of the fluid minus small circles at the locations of the vortices.) The vortices are shed at discrete time instants from the trailing edge of the fish. When this happens, an exchange of momentum ensues and the fish is capable of moving forward. By periodically varying $\dot{\zeta}_y$ — the single input to the system — in a certain way, the fish will move forward or turn.

The model presented in [22], [11] spans the gap between studies which look at deformable bodies moving through a fluid without the use of vortex shedding and studies examining systems with rigid bodies and vortices. Through the model in [22], the authors successfully address motion planning problems for fish locomotion, using only one input and exploiting the presence of vortices for both propulsion and steering.

Next, we first summarize the equations of motion for the fish foil, though we do not rederive these equations. After discussing the basic gaits to move forward and to turn, we then present our control law which allows the fish to move both to a desired location and along a specific path.

A. ODE Model With an Infinite Dimensional Output Map for a Joukowski foil fish in a Potential Flow with Point Vortices

The continually growing number of state variables of this system are

$$\Xi = \left[\zeta_y\ g\ \Lambda^T\ \Gamma^T\right]^T \quad (4)$$

where $g = [\theta_f\ f_x\ f_y]^T$, $\Lambda = [\zeta_1\ \zeta_2\ ...]^T$, with $\zeta_k \in \mathbb{C}^N$, is a vector of the location of each point vortex and $\Gamma = [\gamma_1\ \gamma_2\ ...]^T$, with $\gamma_k \in \mathbb{R}$, is a vector of the strength of each point vortex. The variables θ_f and (f_x, f_y) are the orientation and location of the foil fish with respect to the spatially fixed frame. The number of vortices N continues to grow as time goes on; at periodic discrete points in time another vortex is added. The system has one input, $\dot{\zeta}_y = \Psi$ while the output map defines the potential field and is given in the infinite dimensional form $\phi(x, y) = \eta[\Xi, \Psi](x, y)$. To complete the model description we must develop expressions for the evolution of all the state variables and define the output operator η.

Both [22] and [11] develop the equations of motion for a Joukowski foil in a perfect fluid with point vortices. Reference [11] develops the expression for the potential function which [22] uses (and therefore we use as well). However, [11] uses Newton's second law to derive the motion of the body, while [22] applies conservation laws. Though the two methods should produce the same equations of motion, the simulation results are quite different. We use the motion derived by [22], as in this work, the fish model (correctly) cannot propel itself forward without the inclusion of vortices.

The complex potential $W(z) = \phi(z) + i\psi(z)$ is an analytic function where ϕ is the potential function and ψ is the stream function. We use a frame of reference attached to the foil and we express $W(z)$ in terms of the body configuration and velocities as

$$\begin{aligned} w(\zeta) = W(z) = {} & U w_1(\zeta) + V w_2(\zeta) + \Omega w_3(\zeta) \\ & + \dot{\zeta}_x w_{s1}(\zeta) + \dot{\zeta}_y w_{s2}(\zeta) + \dot{\alpha} w_{s3}(\zeta) \\ & + \sum_{k=1}^{N} w_{pv}^k(\zeta) \end{aligned} \quad (5)$$

where U, V are the translational velocities of the foil, Ω is the rotational velocity, N is the number of vortices in the flow and $w_{pv}^k(\zeta)$ represents the contribution to the potential from the k-th vortex. As noted in [22], the subscript 's' appears in conjunction with variables describing the shape of the foil. Finding the functions w_i and w_{si} corresponds to satisfying the boundary condition that the normal component

of the fluid velocity must match the normal component of the velocity of the foil at its surface. The velocity of the foil at its surface is a combination of the translational and rotational velocities of the foil *plus* the velocities associated with the change in shape $\dot{\zeta}_x, \dot{\zeta}_y, \dot{\alpha}$, which depends on the input $\Psi = \dot{\zeta}_y$. The functions w_{pv}^k are found using the *Milne-Thomson circle theorem* [13]

$$w_{pv}^k = i\gamma_k \left(\log(\zeta - \zeta_k) - \log\left(\zeta - \frac{r_c^2}{\overline{\zeta_k}}\right)\right) \quad (6)$$

where ζ_k is the location of the k-th point vortex, and γ_k is its strength.

Using the complex potential $W(z)$, the kinetic energy of the fluid can be determined from the integral

$$T_f = -\frac{1}{2}\int_{\partial S} \phi(\nabla\phi \cdot \mathbf{n}) ds \quad (7)$$

where ∂S is the surface of the foil. Given that ϕ is a function of the body configuration, the body velocities and the point vortices, T_f can be expressed as

$$T_f = \frac{1}{2}[\mathbf{U}^T \ \dot{\mathbf{s}}^T \ \Gamma^T] \begin{bmatrix} \quad \mathbb{M}^{T_f} \quad \end{bmatrix} \begin{bmatrix} \mathbf{U} \\ \dot{\mathbf{s}} \\ \Gamma \end{bmatrix} \quad (8)$$

$$\mathbf{U} = [\Omega \ U \ V]^T \quad (9)$$

$$\mathbf{s} = [\zeta_x \ \zeta_y \ \alpha]^T \quad (10)$$

$$\Gamma = [\gamma_1 \ ... \ \gamma_N]^T \quad (11)$$

where the body shape $\mathbf{s}(\zeta_y)$ can be determined from ζ_y alone, the matrix $\mathbb{M}^{T_f}(\mathbf{s}, \Lambda)$ depends only on the foil *shape* $\mathbf{s}(\zeta_y)$ and the location of the vortices and the change in body shape $\dot{\mathbf{s}}(\mathbf{s}, \Psi)$ depends only the shape $\mathbf{s}(\zeta_y)$ and the input Ψ. The relationship between ζ_y and ζ_x, a is defined as

$$\zeta_x(\zeta_y) = \frac{(1-\mu)}{(1+\mu)}\sqrt{r_c^2 - \zeta_y^2} \quad (12)$$

$$\alpha(\zeta_y) = \zeta_x - \sqrt{r_c^2 - \zeta_y^2} = -\frac{2\mu}{(1+\mu)}\sqrt{r_c^2 - \zeta_y^2} \quad (13)$$

where $\mu \in (0, 1)$ is a constant. The kinetic energy of the foil can also be expressed in term of the body configuration and velocities

$$T_{\mathcal{B}} = \frac{1}{2}[\mathbf{U}^T \ \dot{\mathbf{s}}^T] \begin{bmatrix} \quad \mathbb{M}^{T_{\mathcal{B}}} \quad \end{bmatrix} \begin{bmatrix} \mathbf{U} \\ \dot{\mathbf{s}} \end{bmatrix} \quad (14)$$

where the matrix $\mathbb{M}^{T_{\mathcal{B}}}(\mathbf{s})$ depends on only the shape $\mathbf{s}$ of the foil. The total effective momentum of the system is

$$A = \frac{\partial(T_{\mathcal{B}} + T_f)}{\partial\Omega} - \frac{1}{2}\sum_{k=1}^{N}(-2\pi\gamma_k)(|\mathbf{z}_k|^2 - |\mathbf{z}_0|^2) \quad (15)$$

$$\mathbf{L} = \begin{bmatrix} \frac{\partial(T_{\mathcal{B}}+T_f)}{\partial U} \\ \frac{\partial(T_{\mathcal{B}}+T_f)}{\partial V} \end{bmatrix} + \sum_{k=1}^{N}(-2\pi\gamma_k)(\mathbf{z}_k + \mathbf{z}_0) \times \mathbf{k} \quad (16)$$

where the terms due to the vortices are developed in [17], $\mathbf{z}_k = [\Re\{z_k\} \ \Im\{z_k\}]^T$ is the vector location of the k-th vortex in the foil-fixed frame, and $\mathbf{z}_0$ is the location of the origin of the foil-fixed frame with respect to the spatially-fixed frame. The momentum is governed by (1)–(2) and the system starts from rest; therefore $\mathbf{L} = [L_x \ L_y]^T = 0$ and $A = 0$ for all time. Thus we have a system of equations

$$\begin{bmatrix} A \\ L_x \\ L_y \end{bmatrix} = I \begin{bmatrix} \Omega \\ U \\ V \end{bmatrix} + B \begin{bmatrix} \dot{\zeta}_x \\ \dot{\zeta}_y \\ \dot{\alpha} \end{bmatrix} + P \begin{bmatrix} \gamma_1 \\ \vdots \\ \gamma_N \end{bmatrix} \quad (17)$$

with a solution

$$\mathbf{U}(\Xi, \Psi) = -I^{-1}\left(B\dot{\mathbf{s}} + P\Gamma\right) \quad (18)$$

where the matrices $I(\mathbf{s})$ and $B(\mathbf{s})$ depend only on the foil shape $\mathbf{s}$ and the matrix $P(\mathbf{s}, \Lambda)$ depends on the shape plus the locations of the vortices.

The remaining two items to summarize are 1) the motion of the point vortices and 2) how to add vortices. The motion of the vortices

$$\dot{\zeta}_k = p_k(\Xi, \Psi) = \left(\overline{\frac{dW_k}{dz}} - (U + iV + i\Omega z_k) - \frac{\partial F}{\partial \zeta_c}\dot{\zeta}_c - \frac{\partial F}{\partial \alpha}\dot{\alpha}\right)\frac{1}{F'(\zeta_k)} \quad (19)$$

$$W_k(z) = W(z) - i\gamma_k \log(z - z_k) \quad (20)$$

is stated in [22] and is found using *Routh's rule* [15]. The point vortices are added to the system one by one at discrete points in time. The trailing edge of the foil (i.e. the stagnation point) is $(\alpha - \zeta_c)$ [22], while we choose the location of the new point vortex as $\zeta_n = 1.5(\alpha - \zeta_c)$. A review of different vortex locating methods (including simulations) can be found in [22]. The condition

$$\frac{dw}{d\zeta}\Big|_{\zeta=\zeta_n} = 0 \quad (21)$$

must be satisfied to guarantee the stagnation point. The addition of the new vortex causes the effective fluid momenta to change, and thus the body momentum must change as well. The discrete change in $\mathbf{U}$, denoted as $\Delta\mathbf{U}$, plus the strength of the new vortex γ_n must satisfy

$$I\Delta\mathbf{U} + P\gamma_n = 0 \quad (22)$$

to ensure the conservation of momentum.

The calculation of $\mathbf{U}$ is split into 1) intervals of time where (17) is used to find the body's translational and rotational velocities due to the body configuration and its shape velocities and 2) points in time where (21) and (22) are used to calculate the discrete change in the body velocities.

Thus, the complete dynamic system is given by the evolution equation

$$\dot{\Xi} = \begin{bmatrix} \dot{\zeta}_y \\ \dot{g} \\ \dot{\Lambda} \\ \dot{\Gamma} \end{bmatrix} = \begin{bmatrix} \Psi \\ l(\Xi, \Psi) \\ \Pi(\Xi, \Psi) \\ 0 \end{bmatrix} \quad (23)$$

and by the infinite dimensional output map

$$\phi(x, y) = \eta[\Xi, \Psi](x, y) = \Re\Big\{W(z)\Big\}, \quad (24)$$

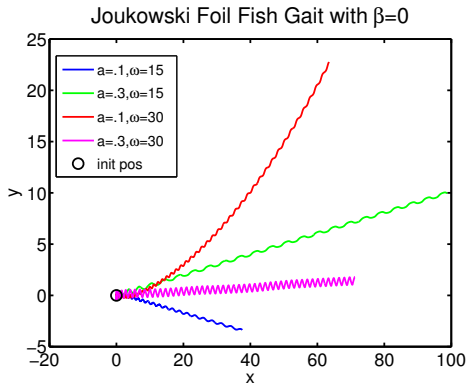

Fig. 1. Forward gait for Joukowski foil fish. $\beta = 0$.

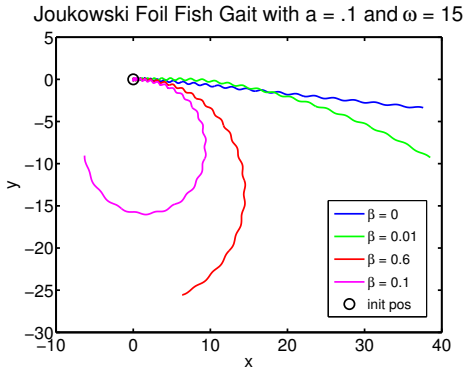

Fig. 2. Turning gait for Joukowski foil fish. $a = .1$, $\omega = 15$.

where

$$\Pi(\Xi,\Psi) = [p_1(\Xi,\Psi)\ p_2(\Xi,\Psi)\ ...]^T \quad (25)$$

$$l(\Xi,\Psi) = \begin{bmatrix} 1 & 0 & 0 \\ 0 & \cos(\theta_f) & -\sin(\theta_f) \\ 0 & \sin(\theta_f) & \cos(\theta_f) \end{bmatrix} \mathbf{U}(\Xi,\Psi)\,, \quad (26)$$

and where $\mathbf{U}(\Xi,\Psi)$ is defined in (18), $p_k(\Xi,\Psi)$ is defined in (19), and $W(z)$ is defined in (5). The initial condition for Λ is arbitrary, while the initial condition for Γ is zero. In this way, until a vortex is initialized, it has no effect on the system. To initialize, each ζ_k in Λ and γ_k in Γ are reset at time $k\Delta t$ where Δt is the time between each shed vortex. Thus the reset is defined as

$$\zeta_k(k\Delta t) = 1.5\Big(\alpha(k\Delta t) - \zeta_c(k\Delta t)\Big) \quad (27)$$

$$\gamma_k(k\Delta t) = \nu_k \quad (28)$$

where ν_k is the γ_n part of the solution to (21), (22) at time $k\Delta t$ where $\zeta_n = \zeta_k$ and $\Delta\mathbf{U}$ is added to (18) for use in (26).

B. Basic Gaits of the Joukowski Foil Fish

As shown in [22], the Joukowski foil fish, with the help of the shed vortices, will move forward and turn with the same input

$$\dot{\zeta}_y = a\omega\cos(\omega t)\,, \quad (29)$$

where the other shape parameters follow from the choice of ζ_y as seen in (12), (13). The difference between the two gaits lies in the initial condition of ζ_y; The fish will move straight forward with the initial condition $\zeta_y|_{t=0} = 0$ while the fish will move around circles with the initial condition $\zeta_y|_{t=0} = \beta$ with $\beta \neq 0$ leading to

$$\zeta_y(t) = a\sin(\omega t) + \beta\,. \quad (30)$$

Figures 2 and 1 show the fish moving forward and in a circle for various choices of parameters. Figure 2 clearly shows the effect of the non-decaying vortices — the fish tail still moves with the same frequency, yet the period of resulting fish locomotion increases. Figure 3 shows snapshots in time of the fish moving forward and the vortices that form.

C. Source Seeking for a Joukowski Foil Fish

We notice that the forward gait and turning gait both have a sinusoidal term. We make β from (30) time dependent and arrive at

$$\dot{\zeta}_y = a\omega\cos(\omega t) + c\xi\sin(\omega t) \quad (31)$$

$$\xi = H(s)[J] \quad (32)$$

$$H(s) = \left(\frac{s}{s+h}\right)^2 \quad (33)$$

where our compensator $H(s)$ is a double washout filter. The function J we wish to maximize is

$$J = -q_r\Big(\big(x^* - f_{sx}\big)^2 + \big(y^* - f_{sy}\big)^2\Big) \quad (34)$$

$$f_s = \left(\mu + \frac{a^2}{\mu}\right)e^{j\theta_f} + f_x + if_y \quad (35)$$

where $f_s = (f_{sx}, f_{sy})$ is the location of the fish sensor, a forward point of the fish — its "nose". As before (x^*, y^*) is the goal location. Figures 4 and 5 depict the fish going toward a target under the influence of (31) and different parameter choices.

We constrain both the value of β and its time derivative $\dot{\beta}$ in the control law of the Joukowski foil fish. We do this both for physical realism and for computational convergence.

D. Path Following for a Joukowski foil fish.

We modify the function J so that the Joukowski foil fish follows a predetermined path. Figure 6 shows the path the fish takes when following the path defined by

$$J = 300/\sqrt{1+\Big|f_x-(3/1000f_y^3-4/15f_y^2+16/3f_y+1)\Big|} \quad (36)$$

IV. Conclusions

We have shown that the extremum seeking method, which performs real-time optimization using periodic perturbations, can perform navigation of underwater vehicles which move through sinusoid-dominated body movement instead of through the use of traditional motors. The algorithm allows the fish to find the source of a signal, move to a target waypoint and follow a prespecified path. These tools can

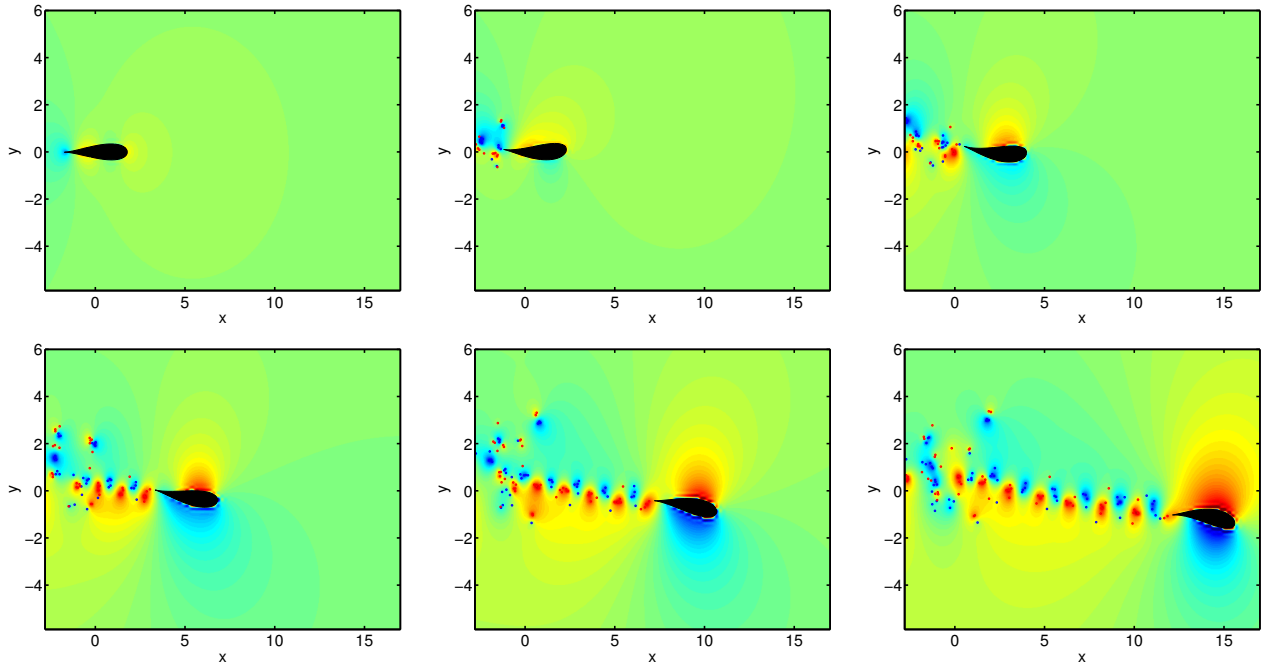

Fig. 3. Snapshots in time of a Joukowski foil fish moving forward. The background color field represents the stream function ψ with red representing positive (clockwise) values and blue negative (counterclockwise). Vortices are also shown as xs moving counter clockwise and os clockwise. $a = .1$, $\beta = 0$.

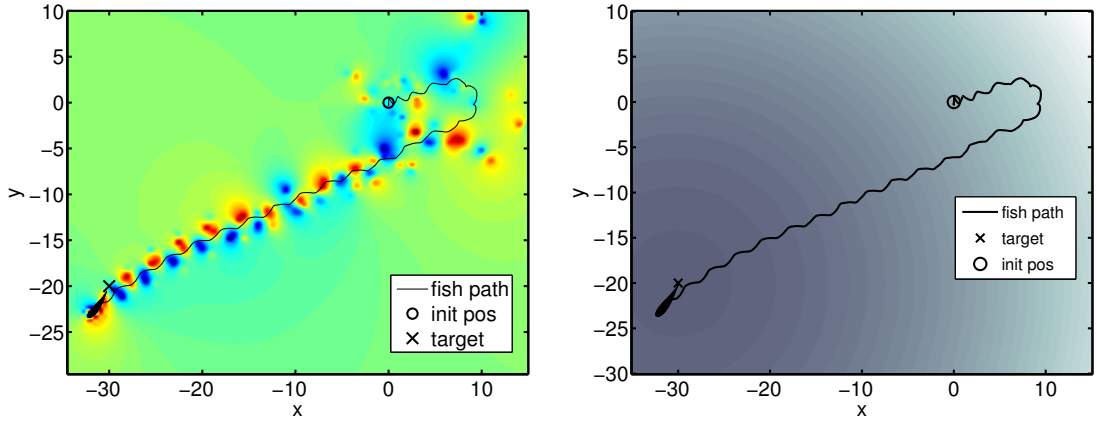

Fig. 4. Source seeking for a Joukowski foil fish. (a) The background color field represents the stream function ψ with red representing positive values and blue negative. (b) The background color field represents the "concentration" of the signal field J with the darker shade representing higher values than the lighter shade. $a = 0.3$, $c = 0.3$, $\omega = 20$, $h = 10$, $q_r = 10.2$, $r_c = 1$, $\mu = 0.74$.

also be used to guide the vehicle through an obstacle field. In so much as the model considered is a realistic model of body-fluid interaction taking place in locomotion of actual fish, the simple control law (31)–(33) seems as a plausible feedback strategy that actual fish may be using to navigate gradient fields.

References

[1] P. W. Bearman, "Vortex shedding from oscillating bluff bodies," *Annu. Rev. Fluid Mech.*, vol. 16, pp. 195–222, 1984.

[2] J. Cochran, E. Kanso, and M. Krstic, "Source seeking for a three-link model of fish locomotion," submitted to *2009 American Control Conference*.

[3] J. Cochran and M. Krstic, "Nonholonomic source seeking with tuning of angular velocity," *IEEE Trans. Automatic Control*, to appear.

[4] J. Cochran, A. Siranosian, N. Ghods, and M. Krstic, "3D source seeking for underactuated vehicles without position measurement," *IEEE Trans. Robotics*, to appear.

[5] J. D. Eldridge, "Numerical simulation of the fluid dynamics of 2D rigid body motion with the vortex particle method," *Journal of Computational Physics*, vol. 221, pp. 626–648, 2007.

[6] J. Gray, "Studies in animal locomotion: VI. the propulsive powers of the dolphin," *J. Experimental Biology*, vol. 13, pp. 192–199, 1936.

[7] E. Kanso, J. E. Marsden, C. W. Rowley, and J. B. Melli-Huber, "Locomotion of articulated bodies in a perfect fluid," *Journal of Nonlinear Science*, vol. 15, pp. 255–289, 2005.

[8] S. D. Kelly and R. B. Hukkeri, "Mechanics, dynamics, and control of a single-input aquatic vehicle with variable coefficient of lift," *IEEE*

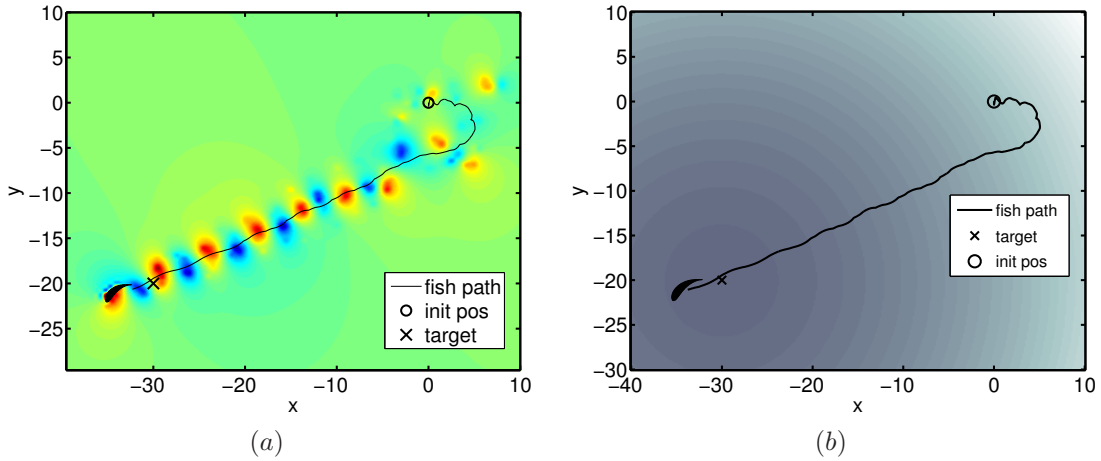

Fig. 5. Source seeking for a Joukowski foil fish. (a) The background color field represents the stream function ψ with red representing positive values and blue negative. (b) The background color field represents the "concentration" of the signal field J with the darker shade representing higher values than the lighter shade. $a = 0.3$, $c = 0.3$, $\omega = 10$, $h = 10$, $q_r = 10.2$, $r_c = 1$, $\mu = 0.74$.

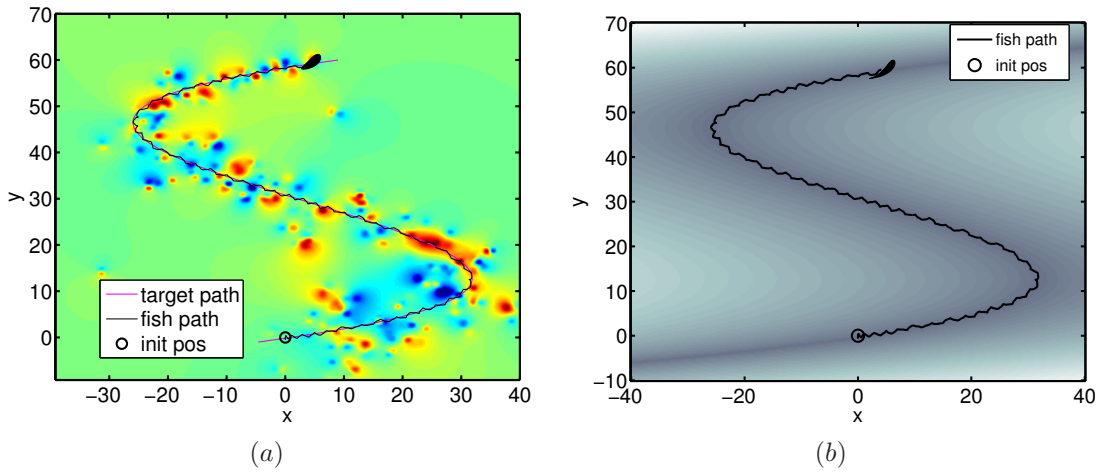

Fig. 6. Joukowski foil fish following a predetermined path. (a) The background color field represents the stream function ψ with red representing positive values and blue negative. (b) The background color field represents the "concentration" of the signal field J with the darker shade representing higher values than the lighter shade. $a = 0.3$, $c = 10$, $\omega = 20$, $h = 20$, $r_c = 1$, $\mu = 0.74$.

Trans. Robotics, vol. 22, no. 6, pp. 1254–1264, 2006.

[9] S. J. Lighthill, *Mathematical Biofluiddynamics*. SIAM, 1975.

[10] P. F. Linden and J. S. Turner, "'optimal' vortex rings and aquatic propulsion mechanisms," *Proc. Royal Soc. Lond. B.*, vol. 241, pp. 647–653, 2004.

[11] R. J. Mason, *Fluid Locomotion and Trajectory Planning for Shape-Changing Robots*. PhD thesis, California Inst. Technology, 2002.

[12] E. Mbemmo, Z. Chen, S. Shatara, and X. Tan, "Modeling of biomimetic robotic fish propelled by an ionic polymer-metal composite actuator," *IEEE International Conf. on Robotics and Automation*, 2008.

[13] L. M. Milne-Thomson, *Theoretical Hydrodynamics*. Dover, 1996.

[14] K. Morgansen, V. Duindam, R. Mason, J. Burdick, and R. Murray, "Nonlinear control methods for planar carangiform robot fish locomotion," *Proc. IEEE Inter. Conf. on Robotics and Automation*, 2001.

[15] P. K. Newton, *The N-vortex problem*. Springer-Verlag, 2001.

[16] B. Protas, "Center manifold analysis of a point-vortex model of vortex shedding with control," *Physica D*, vol. 228, pp. 179–187, 2007.

[17] B. N. Shashikanth, J. E. Marsden, J. W. Burdick, and S. D. Kelly, "The Hamiltonian structure of a 2-D rigid circular cylinder interacting dynamically with N point vortices," *Physics of Fluids*, vol. 14, pp. 1214–1227, 2002.

[18] G. Taylor, "Analysis of the swimming of long and narrow animals," *Proc. Royal Soc. Lond. A.*, vol. 214, no. 1117, pp. 158–183, 1952.

[19] M. S. Triantafyllou and G. S. Triantafyllou, "An efficient swimming machine," *Scientific American*, vol. 272, pp. 64–70, March 1995.

[20] M. S. Triantafyllou, G. S. Triantafyllou, and D. K. P. Yue, "Hydrodynamics of fishlike swimming," *Annu. Rev. Fluid Mech.*, vol. 32, pp. 33–53, 2000.

[21] E. D. Tytell and G. V. Lauder, "The hydrodynamics of eel swimming I. wake structure," *J. Experim. Biology*, vol. 207, pp. 1825–1841, 2004.

[22] H. Xiong, "Geometric mechanics, ideal hydrodynamics, and the locomotion of planar shape-changing aquatic vehicles," 2007.